NMR Spectroscopic Analysis of the DNA Conformation Induced by the Human Testis Determining Factor SRY[†,‡]

Milton H. Werner,[§] Marco E. Bianchi,[||] Angela M. Gronenborn,*,[§] and G. Marius Clore*,[§]

Laboratory of Chemical Physics, Building 5, National Institute of Diabetes and Digestive and Kidney Diseases, National Institutes of Health, Bethesda, Maryland 20892-0520, and DIBIT, San Raffaele Scientific Institute, via Olgettina 58, 20132 Milan, Italy

ABSTRACT: The conformation of an eight base pair DNA oligonucleotide duplex bound to the human testis determining factor SRY and the orientation of the protein domain within the complex have been analyzed by a variety of NMR methods which permit the selective observation of protons attached to ^{12}C nuclei in the presence of uniformly enriched $^{13}C/^{15}N$ protein. Qualitative analysis of nuclear and rotating frame Overhauser enhancement spectra at multiple mixing times indicates that the conformation of the SRY-bound DNA is distinct from that of A- and B-DNA, in agreement with the recent three-dimensional structure determination of the complex [Werner, M. W., Huth, J. R., Gronenborn, A. M., & Clore, G. M. (1995) *Cell 81*, 705−714]. Selective observation of intermolecular NOEs between protein and DNA indicates that partial intercalation of a protein side chain occurs between two adenine bases in the DNA octamer. The analysis of structural features by NMR for this unusual DNA conformer and the orientation of the protein domain on the DNA is discussed. The structural features of the DNA complexed to SRY are remarkably similar, but not identical, to those of DNA complexed to the TATA-binding protein (TBP).

Human SRY (hSRY) protein, also known as the human testis determining factor, is a Y-chromosome encoded transcription factor that acts as a genetic switch in gonadal differentiation (Goodfellow & Lovell-Badge, 1993; Gustafson et al., 1994; McElreavey et al., 1993). The DNA-binding domain of hSRY is a member of the HMG-1/2 superfamily of DNA-binding proteins (Sinclair et al., 1990), and the structure of this domain complexed to an eight base pair oligonucleotide duplex derived from the human Müllerian inhibitor substance (MIS)[1] promoter has recently been solved by multidimensional heteronuclear NMR spectroscopy (Werner et al., 1995). Structural and biochemical data suggest that the primary function of hSRY is its ability to dramatically distort the DNA conformation, in particular to cause helix unwinding, minor groove expansion, and bending (Werner et al., 1995). With the exception of SRY-bound DNA, all DNA duplexes analyzed by NMR, either free in solution or in complexes with proteins, have been of the B type. While the pattern of nuclear Overhauser effects for B- and A-DNA are well established [see Clore and Gronenborn (1985) and van De Ven and Hilbers (1988) for reviews], those for a highly distorted conformation such as that found in the SRY-bound DNA are not. In this paper, we therefore present a qualitative analysis of the spectroscopic characteristics of

SRY-bound DNA using heteronuclear-filtered NMR experiments (Otting & Wüthrich, 1990; Ikura & Bax, 1992) which permit the selective observation of DNA protons attached to ^{12}C in the presence of uniformly enriched $^{13}C/^{15}N$ protein. We show that a simple qualitative analysis of the nuclear and rotating frame Overhauser enhancement spectra clearly demonstrates that the conformation of SRY-bound DNA is very different from either classical B- or A-DNA.

EXPERIMENTAL PROCEDURES

Sample Preparation. The hSRY-HMG domain (MQDRVKRPMNAFIVWSRDQRRKMALEN-PRMRNSEISKQLGYQWKMLTEAEKW-PFFQEAQKLQAMHREKYPNYKYR), comprising residues 58−133 of intact hSRY together with an N-terminal Met, was overexpressed in *Escherichia coli* under the control of the T7-lac promoter using uniformly enriched [$^{13}C_6$]glucose and $^{15}NH_4Cl$ as the sole carbon and nitrogen sources, respectively. The protein was purified as described by Ferrari et al. (1992) with the exception of the additon of a phosphocellulose column (linear gradient 0−1.5 M KCl, 10 mM Tris-HCl, pH 7.5) prior to the final purification on Mono-S (linear gradient 0−0.6 M NaCl, 20 mM sodium phosphate, pH 6.5). Purity and homogeneity of the hSRY-HMG domain was assessed by denaturing SDS−polyacrylamide electrophoresis and laser desorption mass spectrometry. Activity was assessed by mobility shift of the MIS binding site as described previously (Ferrari et al., 1992).

Eighteen micromoles of each DNA strand (5'-dGCA-CAAAC and 5'-dGTTTGTGC) was synthesized on an Applied Biosystems 380B DNA synthesizer with trityl groups attached. The crude oligonucleotides were purified by reverse-phase HPLC (0.1 M triethylammonium acetate v. 90% acetonitrile, 0−60% over 30 min, 10 mL/min) and detrylated in 0.1 M glacial acetic acid at 25 °C for 8 h.

The detritylated oligonucleotides were subsequently purified on a Mono-Q column (0–0.3 M NaCl, 10 mM sodium phosphate, 1 mM EDTA, pH 6.5) and annealed by mixing the fractions containing the purified strands in equimolar amounts, heating to 90 °C, followed by slowly cooling to room temperature in a water bath. The crude oligonucleotide duplex was passed over a Mono-Q column (0–0.6 M NaCl, 10 mM sodium phosphate, 1 mM EDTA, pH 6.5) to remove residual single strands. Purity and homogeneity of the duplex was assessed by radiolabeling with ^{32}P and separation by native and denaturing (urea) sequencing gel electrophoresis. Complexes of the hSRY-HMG domain and the MIS DNA binding site were formed by mixing the purified components at room temperature in the ratio 1:0.9 protein to DNA at a final protein concentration of 0.3 mg/mL protein in 10 mM potassium phosphate, pH 6.8. After incubation for 3–5 h, the dilute complex solution was then concentrated in either a colloidian apparatus (Schleicher & Schuell) or a Micro-ProDiCon (Spectrum) to a final volume of 0.25–0.5 mL. The final concentration of protein was determined by the method of Bradford (1976) and for the DNA spectrophotometrically using an extinction coefficient of 50 μg mL^{-1} OD^{-1}. This yielded a ratio of 1:1.05 for protein to DNA in the NMR samples. For samples in D_2O, the complex was dialyzed against three changes of 125 mL of D_2O buffer in a nitrogen atmosphere. The concentration in the final NMR samples ranged from 0.9 to 1.6 mM in complex.

NMR Spectroscopy. All spectra were collected on a Bruker AMX-500 equipped with a shielded z-gradient triple-resonance probe at 37 (D_2O) or 39 (H_2O) or 23 °C (free DNA). In all cases, phase-sensitive spectra were collected using the States–TPPI procedure (Marion & Bax, 1989). Spectra were processed using the nmrPipe software package (F. Delaglio, personal communication) and analyzed with the programs PIPP and CAPP (Garrett et al., 1991). Some of the ^{12}C-filtered NOE, ROE, and J-correlated spectra were collected in H_2O. Water suppression in H_2O was achieved using the Watergate gradient echo pulse train (Piotto et al., 1992) in the case of the ^{12}C/^{14}N-filtered NOE and ROE spectra (Figure 1) and by presaturation of the water resonance in the case of the quantitative J-correlation spectra.

A 2D ^{12}C-filtered HOHAHA spectrum was collected with a mixing time of 39 ms using the pulse sequence of Bax et al. (1994). A data matrix of 300 × 1024 complex data points was recorded with 2 × 32 scans for each complex t_1 increment, a t_{1max} of 51 ms, and a total measuring time of 10 h. The residual HDO signal was suppressed by presaturation with a weak radiofrequency field.

2D ^{12}C-filtered NOE spectra were collected with mixing times of 35, 75, and 185 ms either as described previously (Vuister et al., 1994) for D_2O samples or with minor modifications including ^{14}N-filtering (Figure 1a) for H_2O samples. The ^{13}C purging delay was set at 3.57 ms to supress aliphatic and aromatic protons attached to ^{13}C during t_1 and optimized to 3.12 ms to suppress aromatic protons attached to ^{13}C during t_2. Data matrices of either 256 × 1024 or 512 × 1024 complex data points were recorded with 2 × 64 scans per t_1 increment, a t_{1max} of 51 ms and total measuring time of ~23 or ~45 h, respectively.

2D ^{12}C-filtered ROE spectra were collected using a modification of the 2D ^{12}C-filtered NOE sequence of Vuister et al. (1994) in which the NOE mixing period was replaced with a continuous 4.2 kHz spin-lock field of 30 ms duration
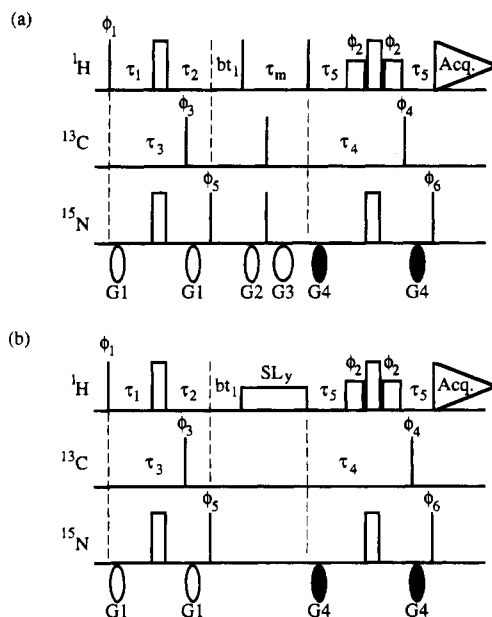

FIGURE 1: Pulse sequences for the 2D ^{12}C/^{14}N-filtered NOE (a) and ROE (b) experiments. In each case, water suppression is achieved by a gradient-echo pulse sequence (Piotto et al., 1992). Narrow pulses have 90° flip angles, wide pulses of equal height have a 180° flip angle, and short wide pulses are selective 90° pulses (1.9 ms in length) applied at the carrier frequency. All pulses are applied along x unless otherwise indicated. Gradients are indicated with an ellipse and are sine-bell shaped, 25 G/cm at the center; the sign of the gradient is positive when shaded black, negative otherwise. In panels a and b, the evolution along t_1 is of the mixed-constant time type (Grzesiek & Bax, 1993) whereby an increasing fraction of the evolution period is incorporated into the $\tau_1 + \tau_2$ ^{12}C-filtering delay. Delay durations for schemes a and b are as follows: $\tau_1 = (1/4J_{NH}) - at_1$, $\tau_2 = (1/4J_{NH}) + at_1$ with $a = (1/4J_{NH})/t_{1max}$ and $b = 1 - 2a$; $\tau_3 = (1/2J_{CH})$ with $J_{CH} = 140$ Hz; $\tau_4 = (1/2J_{CH})$ with $J_{CH} = 160$ Hz; $\tau_5 = (1/4J_{NH})$; $\tau_m =$ NOE mixing time; SL = spin lock (4.2 kHz RF field). Phase cycling is as follows: $\phi_1 = x, -x$; $\phi_2 = -x$; $\phi_3 = 8(x), 8(-x)$; $\phi_4 = 16(x), 16(-x)$; $\phi_5 = 2(x), 2(-x)$; $\phi_6 = 4(x), 4(-x)$; acq $= x, -x$. Quadrature in t_1 is obtained using the States–TPPI method (Marion et al., 1989) on ϕ_1. Gradient durations for G1, G2, G3, and G4 are 0.5, 1, 3.5, and 1 ms, respectively.

(Figure 1b). For D_2O samples the residual HOD resonance was suppressed by weak presaturation with frequency jumping from a carrier frequency of 6.56 ppm to the solvent frequency at 4.66 ppm. For H_2O samples, ^{14}N-filtering was also incorporated into the pulse scheme (Figure 1b), the carrier was set at the solvent frequency, and only analysis of ROEs to base protons was carried out. A data matrix of 256 (free DNA) or 512 (bound DNA) × 1024 complex points was collected with 2 × 64 scans per t_1 increment, a t_{1max} of either 44 (bound DNA) or 71.7 ms (free DNA), and a total measuring time of 12–25 h.

Intermolecular NOEs between DNA imino protons and protein protons were derived from a 2D ^{1}H–^{1}H NOE spectrum recorded in H_2O with a 150 ms mixing time using a binomial 1-1 solvent suppression sequence (Plateau & Guéron, 1982). A data matrix of 400 × 1024 complex points was collected with 2 × 64 scans for each complex t_1 increment, a t_{1max} of 18.5 ms, and a total measuring time of 36 h.

Intermolecular NOEs between protein sidechain protons (attached to ^{13}C) and DNA protons (attached to ^{12}C) were obtained from a 3D ^{13}C-edited (F$_2$)/^{12}C-filtered (F$_3$) NOE spectrum recorded with a 155 ms mixing time (Vuister et
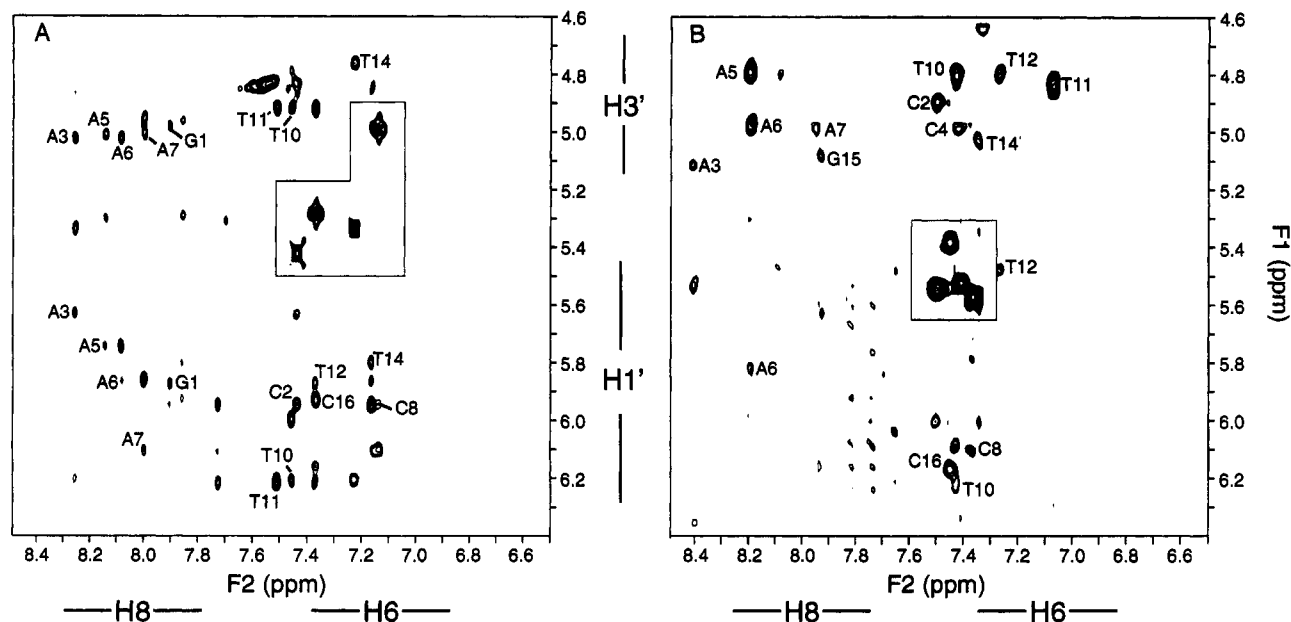
FIGURE 2: Portion of the 2D ^{12}C-filtered NOE spectra (75 ms mixing time) for (A) free and (B) hSRY-bound DNA. Labels indicate the position of the intraresidue H8/H6–H1′ and H8/H6–H3′ NOE cross peaks. The intraresidue H6–H5 cross peaks for the cytosine bases are boxed in. The two spectra are normalized with respect to sample concentration to permit direct comparison.

al., 1994). The spectrum is the result of a 128 × 16 × 512 complex data point matrix collected with 2 × 16 scans per complex t_1,t_2 increment, a t_{1max} of 10.2 ms, a t_{2max} of 2.6 ms, and total measuring time of about 4 days.

RESULTS

Noncanonical Helix Conformation of SRY-Bound DNA. At a mixing time of 75 ms, the 2D NOE spectrum of the free DNA octamer displays cross peak intensities typical of B-DNA (Figure 2A). Specifically, the intensities of the intraresidue and sequential NOE cross peaks from the base protons to the H1′ and H3′ sugar protons are relatively weak and of comparable intensity (Figure 2A). These observations are consistent with the 3.5–4 Å distance between these protons in B-form DNA and can be compared to the strong cross peaks observed between the H5 and H6 protons in the pyrimidine ring of cytosine which are fixed at a distance 2.4 Å. In stark contrast, the 75 ms 2D NOE spectrum of the protein-bound DNA displays vanishing intensities for the intraresidue and sequential NOE cross peaks between the H1′ sugar and H8/H6 base protons, while most of the intraresidue H3′ to H6/H8 cross peaks are unusually intense (Figure 2B). These observations suggest that the DNA conformation possesses some A-like character (Clore & Gronenborn, 1985; van de Ven & Hilbers, 1988).

Further analysis of NOE cross peak intensities involving the base protons and deoxyribose H2′ and H2″ protons, however, suggests that the protein-bound DNA in fact represents a confomer unlike either canonical A- or B-DNA. Thus an A-like structure should be manifested by very strong sequential H2′(i)–H6/H8(i+1) NOEs and weak intraresidue H2′(i)–H6/H8(i) NOEs; a B-like confomer, on the other hand, should display strong intraresidue H2′(i)–H6/H8(i) NOEs and strong sequential H2″(i)–H8/H6(i+1) NOEs (Clore & Gronenborn, 1985; van de Ven & Hilbers, 1988). Figure 3 illustrates that while the free DNA displays the expected pattern of NOE intensities for B-DNA (Figure 3A), the SRY-bound DNA exhibits features distinct from both

typical A- and B-like conformations (Figure 3B). In particular, the sequential H2″(i)–H8/H6(i+1) NOEs are very weak and the sequential H2′(i)–H8/H6(i+1) NOEs are vanishingly small, while the intraresidue H2′(i)–H8/H6(i) NOEs are strong (Figure 3B). These data in conjunction with NOE observations involving H1′ and H3′ sugar protons strongly suggest a noncanonical DNA conformation. The relevant NOE patterns for these three different DNA conformations are schematically illustrated in Figure 4.

Spin-diffusion via the H2′/H2″ geminal pair can significantly affect the observed relative intensities of the H8/H6–H3′ and H8/H6–H1′ NOEs, often making them appear more intense than would be expected from the molecular structure of B-form DNA (Bauer et al., 1990). To ascertain the effects of spin diffusion on the above observations, we recorded a number of 2D ROE spectra. In these spectra direct ROE peaks are positive (that is of opposite sign to the diagonal) while cross peaks dominated by spin-diffusion are negative (that is of the same sign as the diagonal) (Bax & Davis, 1985). Only one negative intraresidue base–H2′/H2″ ROE is observed, namely, that between the H8 and H2″ of T12 (Figure 5). In addition, nearly all the intraresidue H8/H6–H1′, H8/H6–H3′, H1′–H2′/H2″, and H2′/2″–H3′ are positive with the exception of the intraresidue H6–H3′, H1′–H2″, and H1′–H2′ ROEs for C8, A3, and C2, respectively, which are negative. Semiquantitative analysis of 35, 75, and 185 ms NOE spectra (data not shown) shows that the relative intensities of the intraresidue and sequential NOE cross peaks as a function of mixing time follow the same trends seen in ROE spectra for the free and bound DNA. These observations indicate that spin-diffusion does not play a prominent role in the unusual observations described above for SRY-bound DNA.

Atypical NOEs between Sequentially Related Protons. A number of NOE connectivities were observed in the bound DNA between sequentially related protons that are not typically observed in B-form DNA. These included sequential CH₃(i)–H6/H8(i+1) NOEs for the methyl groups of T10,
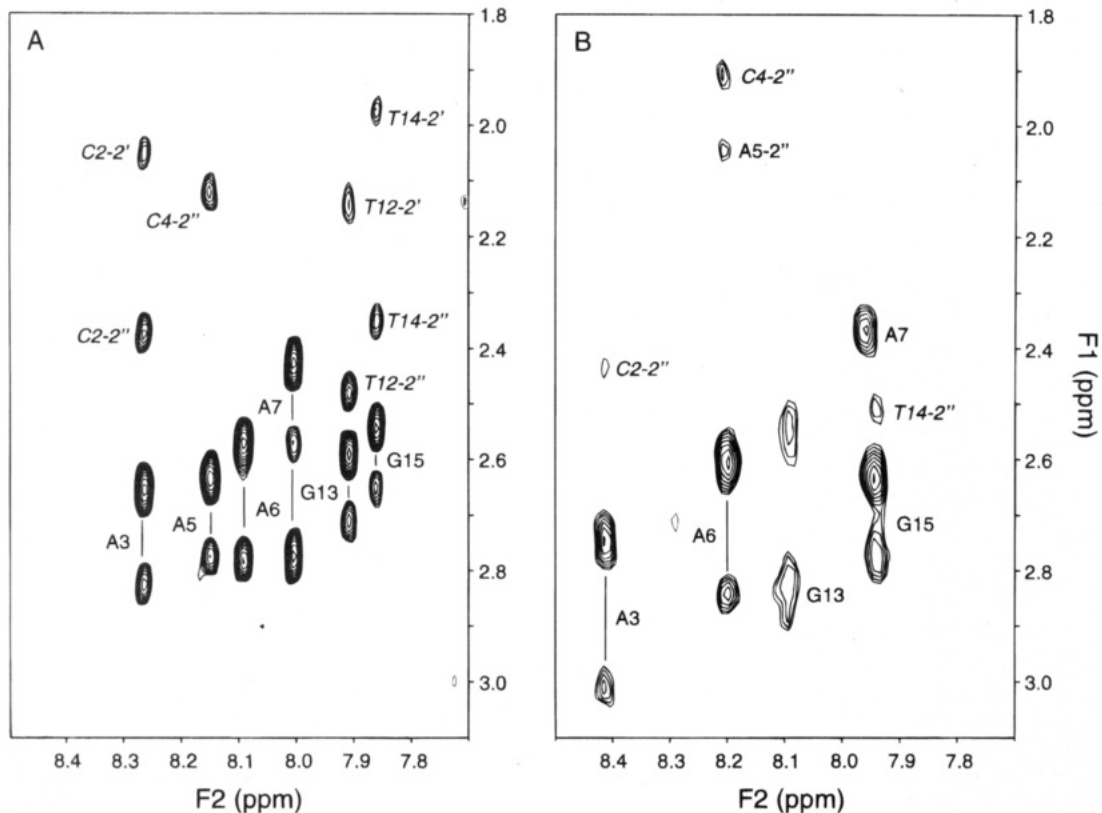
FIGURE 3: Portion of the 2D ^{12}C-filtered NOE spectra (75 ms mixing time) of (A) free and (B) hSRY-bound DNA illustrating the relative intensity of the H8/H6−H2′/H2″ NOEs. The H2′ resonances are upfield of the corresponding H2″ resonances except for A7 in panel B where the H2′ and H2″ resonances are degenerate. Sequential NOEs from the preceding residue are labeled in italics. The two spectra are normalized with respect to sample concentration to permit direct comparison.
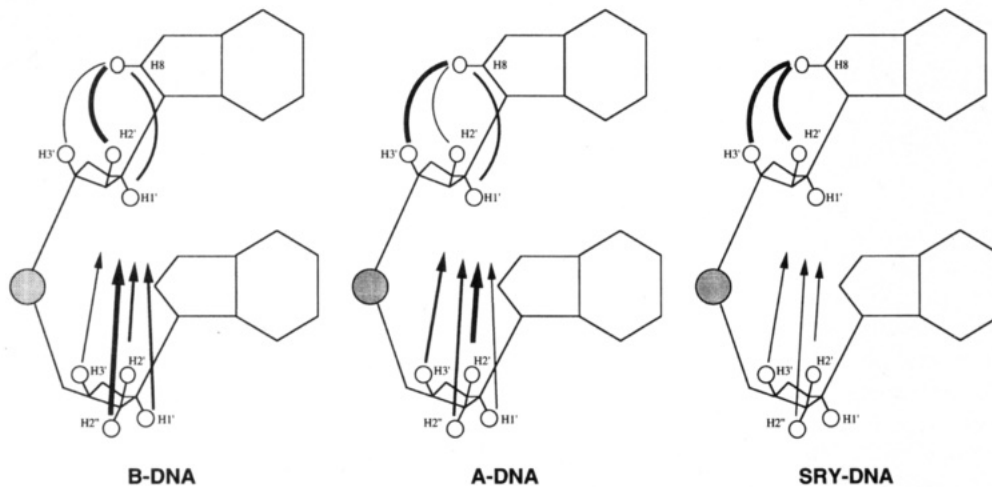

FIGURE 4: Schematic representation of the relative NOE intensities at ≤75 ms mixing time observed for the free DNA octamer (which is B form) and the SRY-bound DNA octamer and expected for classical A DNA. Curves indicate intraresidue contacts, and arrows indicate sequential contacts between the previous deoxyribose proton and the next base proton (H8 in the figure). The thin, medium, and thick lines indicate weak to very weak, medium, and strong intensities, corresponding to interproton distances >4 Å, 2.5−4 Å and <2.5 Å, respectively. For SRY-bound DNA, intraresidue and sequential NOEs involving the H1′ sugar and H8/H6 base protons had vanishing intensity and no lines or arrows are shown.

T11, T12, and T14; sequential H1′(*i*)−H1′(*i*+1) NOEs between C4 and A5, G9 and T10, and T10 and T11; sequential H1′(*i*)−H5(*i*+1) NOEs between G1 and C2, A3 and C4, and G15 and C16; sequential H2(*i*)−H1′(*i*+1) NOEs between A3 and C4, and A7 and C8. Sequential H3′(*i*)−H5/CH$_3$(*i*+1) NOEs were also observed between A7 and C8, G9 and T10, T10 and T11, T11 and T12, and G15 and C16, as were unusually strong sequential CH$_3$(*i*)−CH$_3$(*i*+1) NOEs between T10 and T11, and T11 and T12.

The H3′(*i*)−H5/CH$_3$(*i*+1) and H2(*i*)−H1′(*i*+1) NOEs, as well as the moderately intense CH$_3$(*i*)−CH$_3$(*i*+1) NOEs, would be expected to be seen in an A-like DNA conformer. The sequential methyl to base, H3′ to H5/methyl, and very strong methyl to methyl NOEs, however, are unique to this DNA conformer. None of these NOEs are observed in spectra of the free DNA, even at a mixing time of 250 ms.

Intermolecular NOEs between Protein and DNA. The unusual DNA conformation gleaned from a qualitative
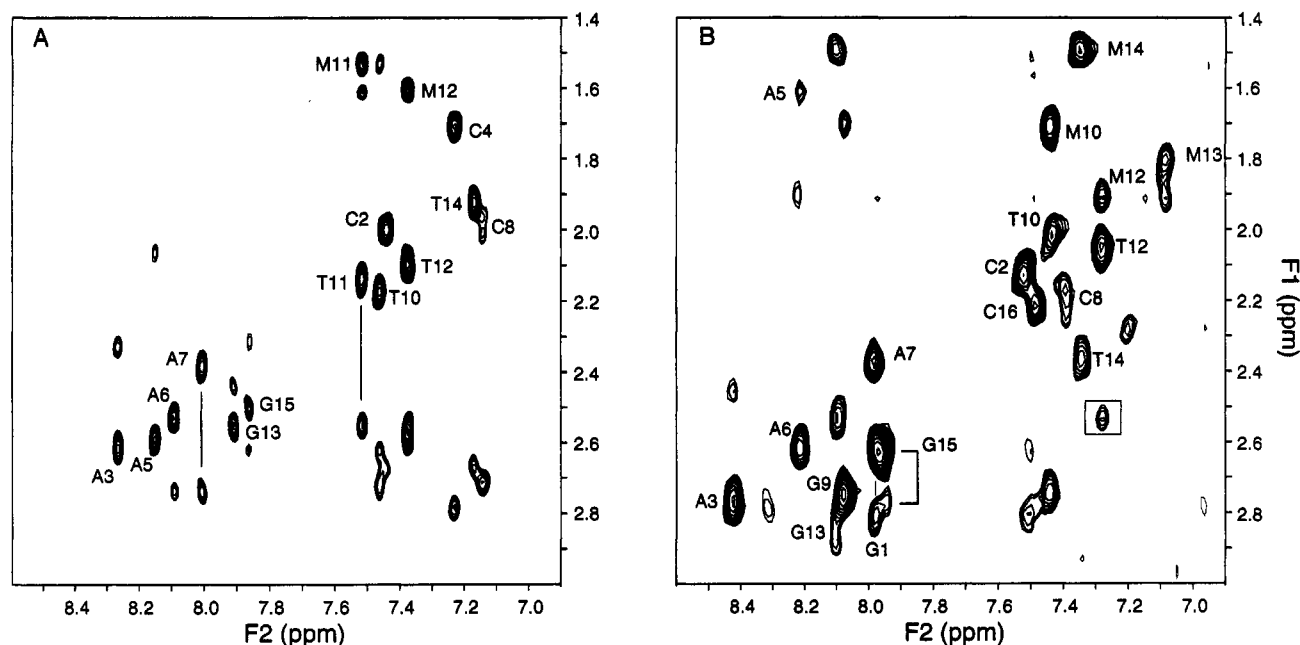
FIGURE 5: Portion of the 2D ^{12}C-filtered ROE spectra (30 ms mixing time) of (A) free and (B) SRY-bound DNA. Labels in each spectrum indicate the H8/H6−H2′ cross peak; M refers to the C5-methyl group of thymidine. The H2′ resonances are upfield of the corresponding H2″ ones except for A7 in panel B where the H2′ and H2″ resonances are degenerate. Contours are positive except for the intraresidue H6−H2″ cross peak for T12 (indicated by the square box). The spectrum in B was collected in H_2O at 39 °C using the pulse sequence given in Figure 1B. The chemical shifts for the indicated peaks are therefore slightly different than those in Figures 2 and 3 which were recorded at 37 °C.

analysis of the NOE and ROE data of SRY-bound DNA is supported by the observation of numerous NOEs between SRY and the DNA exclusively in the minor groove. Specifically, a homonuclear ^{1}H−^{1}H NOE experiment in H_2O permitted direct observation of NOEs between the side chain of Ile13 and the imino protons of base pairs 5 and 6 (Figure 6, top). The observation of these NOEs in a previous NMR analysis (King & Weiss, 1993; Haqq et al., 1994) led to the suggestion of partial intercalation of this side chain at the TpT step in the DNA. In fact, in our structure (Werner et al., 1995) the partial intercalation of Ile13 is seen to occur between the ApA step of base pairs 5 and 6 of the DNA octamer. Thus NOEs are observed between the side chain protons of Ile13 and the adenine base and deoxyribose protons of A5 and A6 (Figure 6, bottom). These contacts together with the NOEs observed from the side chains of Ile35 and Ser36 to base pairs 7 and 8 of the DNA, and between the aromatic ring of Tyr74 and the adenine base of A3 (Figure 6, bottom), unambiguously define the orientation of the hSRY-HMG domain within the minor groove. Access to the minor groove by multiple regions of SRY necessitate significant distortion in the DNA helix and substantial minor groove widening in order to permit close intermolecular contacts to be observed between SRY and DNA.

DISCUSSION

Circular permutation analyses of sequence-specific HMG DNA-binding domains have suggested that the DNA conformation induced by the binding of the protein domain is significantly distorted from canonical DNA (Giese et al., 1992; Pontiggia et al., 1994). This was confirmed by the structure determination of the complex of the hSRY-HMG with DNA (Werner et al., 1995) which demonstrated that the DNA was severely underwound and bent with expansion of the minor groove and compression of the major groove.

The structure of the complex also suggests that a major contribution to the distortion arises from a "wedge" driven helical unwinding of the DNA caused by the exclusively minor goove binding of hSRY, coupled with the partial intercalation of Ile13 between two adenines at base pairs 5 and 6 of the duplex DNA. The "wedge" driving the unwinding of the DNA is formed by a tetrad of amino acid side chains comprising Met9, Phe12, Ile13, and Trp43. In addition to this localized cause of distortion, the overall conformation of the DNA in the complex is to a large extent driven by the protein's overall shape as manifested by the 75 intermolecular NOE restraints between the protein and DNA (Werner et al., 1995). The role of the 338 approximate loose interproton distance restraints within the DNA itself contribute less to defining the overall structure of the DNA due to the fact that the NOEs within the DNA are limited to adjacent base pairs and hence are poor at defining long range order (Werner et al., 1995).

Comparison of NOE and ROE data of free and bound DNA confirms that evidence for this unusual DNA structure can be directly deduced from a qualitative analysis of short mixing time (≤ 75 ms) NOE data. Analysis of the ROE data demonstrates that spin-diffusion effects did not significantly influence the assessment of the loose approximate interproton distance restraints derived from the NOE experiments on the bound DNA. Although J-coupling can contribute to the ROE intensity via Hartman−Hahn effects (which are of opposite sign to the ROE) in the case of coupled spin systems (e.g., cross peaks between sugar protons), placing the carrier at 6.56 ppm largely suppresses such transfers as the Hartmann−Hahn matching condition is not satisfied during the ROE spin-lock period (Bax, 1988). In addition, no J-coupling exists between base and deoxyribose protons, and hence the ROE intensities between these protons are unaffected by scalar couplings. Thus, there appears to be little contribution
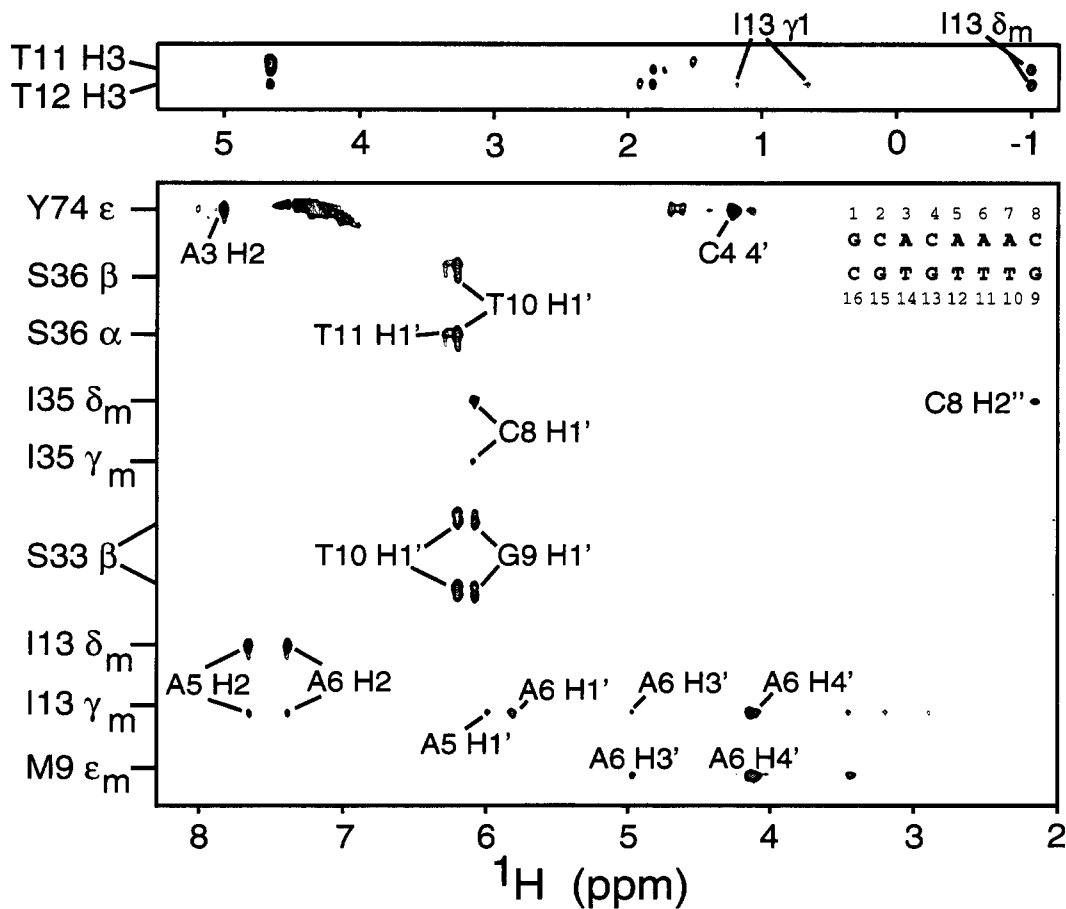
FIGURE 6: Intermolecular NOEs between the hSRY-HMG domain and DNA. (Top) A portion of the 150 ms 2D ^{1}H−^{1}H NOE spectrum demonstrating contacts between the methyl protons of Ile13 and the basepaired imino protons of T11 and T12, illustrating partial intercalation of the side chain of Ile13 between base pairs 5 and 6 in the DNA octamer. (Bottom) Composite of a 3D ^{13}C(F_2)-edited/^{12}C-filtered(F_3) NOE spectrum (155 ms mixing time) illustrating NOE contacts between protein side chains (labeled on left) and DNA protons. The orientation of the protein domain within the minor groove is determined by the NOEs from the side chains of Ile13 and Met9 to the bases and deoxyribose sugars of A5 and A6, from the side chains of Ile35 and Ser36 to base pairs 7 and 8, and from the aromatic ring of Tyr74 to the base of A3 and the deoxyribose sugar of C4. The octamer sequence and numbering convention appear in the upper right-hand corner.

of indirect transfer events on the NOE cross peak intensities in the bound DNA spectra. We therefore conclude that the unusual sequential and intraresidue NOE intensities observed in the bound DNA spectra are a consequence of a significantly distorted DNA conformation upon protein binding.

Diagnostic observations for the underwound DNA structure found in the hSRY-DNA complex are the unusually weak intraresidue and sequential NOEs involving the H1′ sugar protons and the strong intraresidue H8/H6−H3′ and H8/H6−H2′ NOEs of comparable intensity at short mixing times. The fact that the intraresidue H8/H6−H3′ and H8/H6−H2′ NOE/ROE intensities are very strong while the sequential H1′(i)−H8/H6(i+1) and H2′/H2″(i)−H8/H6(i+1) NOE/ROE intensities are very weak (Figure 4) argues that the DNA conformation is neither A- nor B-like but rather something in between. In this regard, it is interesting to note that in those cases where $^3J_{1′−2′}$ coupling constants could be measured by quantitative J-correlation spectroscopy (Vuister et al., 1994), the measured couplings ranged from 3 to 7 Hz (data not shown). These values correspond to more A-like sugar conformations (Kim et al., 1992) but are far from the 1 Hz values of a pure C3′-endo sugar conformation that would be found in canonical A-form DNA. Alternatively, motional averaging of the sugar ring conformation between pure C3′-endo and C2′-endo may occur. Clearly, this is known to occur to some extent in free B-DNA (van de Ven

& Hilbers, 1988; Kim et al., 1992), but it seems less likely to occur in a complex where the flexibility of the deoxyribose may be hindered by interactions with the protein.

Intermolecular NOEs between protein and DNA uniquely define the orientation of the protein within the minor groove of the DNA. Previous observations of NOEs between a single isoleucine methyl group and two thymidine imino protons led to the suggestion that a side chain intercalates between two DNA bases (King & Weiss, 1993; Haqq et al., 1994). These limited observations, however, were inadequate to determine whether the intercalation actually occurs between two thymidine bases or their adenine partners. A more detailed analysis (Figure 6) demonstrates that the partial intercalation of the side chain of Ile13 occurs between A5 and A6, with numerous NOEs observed between Ile13 and both the base and deoyribose protons of these two adenines.

The solution structure of the complex of the hSRY-HMG domain with DNA (Werner et al., 1995) and the crystal structure of TATA-box binding protein (TBP) bound to DNA (Kim, J. L., et al., 1993; Kim, Y., et al., 1993; Kim & Burley, 1994) both display exclusive minor groove binding with concomitant helical unwinding. Comparison of the NMR observations made on the hSRY-DNA complex with the structures of the TBP- and hSRY-DNA complexes illustrates some similarities in the protein-induced DNA distortion. The absence of sequential H1′(i)−H8/H6(i+1) NOEs at short

mixing times is consistent with the 5.5−6 Å distance between these protons in both the TBP-bound DNA and the hSRY-bound DNA. For distances involving the H2′/H2″ protons of the SRY-bound DNA, most of the sequential H2′(i)−H8/H6(i+1) distances range from 3−3.5 Å while the intraresidue H2′−H8 distances are all ∼2.5 Å. Thus, the relative intensities of these cross peaks in the NOE/ROE spectra of the bound DNA are consistent with the distances measured in the structure of the hSRY-DNA complex; these distances also fall in the same ranges in the TBP-DNA crystal structure. In addition, the observed atypical sequential NOEs in the SRY-bound DNA spectra are consistent with the shortening of these distances in these distorted DNA structures. In this regard it is interesting to note that the TBP-bound DNA displays A-like sugar puckers with a tendency toward C4′-exo or O1′-endo just as found for hSRY-bound DNA. These observations support the notion that the distortions in the TBP- and hSRY-bound DNA conformations are similar in character. Indeed, the similarities in the structure of DNA complexed to SRY and TBP may be a reflection of the limited number of DNA conformations compatible with exclusive minor groove binding coupled with the severe bending of the DNA that both proteins produce. The opposite possibility that both proteins bend the DNA in the same way because of similar protein−DNA contacts appears not to be true as the interaction surfaces of SRY and TBP are completely different, namely helices for the former and a 10-stranded antiparallel β-sheet for the latter.

While related, the DNA structures in the hSRY (Werner et al., 1995) and TBP (Kim, J. L., et al., 1993; Kim, Y., et al. 1993; Kim & Burley, 1994) complexes are not identical. TBP-bound DNA is approximately 20% more underwound with interbase roll angles that are approximately 70% larger than that found in hSRY-bound DNA. The minor groove is approximately 10% wider, and the overall bend is approximately 30° less in SRY-bound DNA compared to TBP-bound DNA. None of these differences can be directly ascertained from a qualitative analysis of the NOE spectra.

REFERENCES

Altona, C., & Sundaralingam, M. (1972) *J. Am. Chem. Soc. 94*, 8205−8212.

Clore, G. M., & Gronenborn, A. M. (1985) *Prog. Nucl. Magn. Reson. Spectrosc. 17*, 1−32.

Bax, A. (1988) *J. Magn. Reson. 77*, 134−147.

Bax, A., Grzesiek, S., Gronenborn, A. M., & Clore, G. M. (1994) *J. Magn. Reson., Ser. A 106*, 269−273.

Bradford, M. (1976) *Anal. Biochem. 72*, 248−256.

Ferrari, S., Harley, V. R., Pontiggia, A., Goodfellow, P. N., Lovell-Badge, R., & Bianchi, M. E. (1992) *EMBO J. 11*, 4497−4506.

Garrett, D. S., Powers, R., Gronenborn, A. M., & Clore, G. M. (1991) *J. Magn. Reson. 95*, 214−220.

Giese, K., Cox, J., & Grosschedl, R. (1992) *Cell 69*, 185−195.

Goodfellow, P. N., & Lovell-Badge, R. (1993) *Annu. Rev. Genet. 27*, 71−92.

Grzesiek, S., & Bax, A. (1993) *J. Biomol. NMR 3*, 185−204.

Gustafson, M. L., & Donahoe, P. K. (1994) *Annu. Rev. Med. 45*, 505−524.

Haqq, C. M., King, C.-Y., Ukiyama, E., Falafi, S., Haqq, T. N., Donahoe, P. K., & Weiss, M. A. (1994) *Science 266*, 1494−1500.

Ikura, M., & Bax, A. (1992) *J. Am. Chem. Soc. 114*, 2433−2440.

Kim, J. L., & Burley, S. K. (1994) *Nature Struct. Biol. 1*, 638−653.

Kim, J. L., Nikolov, D. B., & Burley, S. K. (1993) *Nature 365*, 520−527.

Kim, S.-G., Lin, L.-J., & Reid, B. R. (1992) *Biochemistry 31*, 3564−3574.

Kim, Y., Geiger, J. H., Hahn, S., & Sigler, P. B. (1993) *Nature 365*, 512−520.

King, C.-Y., & Weiss, M. A. (1993). *Proc. Natl. Acad. Sci. U.S.A. 90*, 11990−11994.

Marion, D., Ikura, M., Tschudin, R., & Bax, A. (1989) *J. Magn. Reson. 85*, 393−399.

McElreavey, K., Vilain, E., Cotinot, C., Payen, E., & Fellous, M. (1993) *Eur. J. Biochem. 218*, 769−783.

Piotto, M., Saudek, V., & Sklenar, V. (1992) *J. Biomol. NMR 2*, 661−665.

Plateau, P., & Guéron, M. (1982) *J. Am. Chem. Soc. 104*, 7310−7311.

Pontiggia, S., Rimini, R., Varley, V. R., Goodfellow, P. N., Lovell-Badge, R., & Bianchi, M. E. (1994) *EMBO J. 13*, 6115−6124.

Vuister, G. W., Kim, S.-J., Wu, C., & Bax, A. (1994) *J. Am. Chem. Soc. 116*, 9206−9210.

Werner, M. H., Huth, J. R., Gronenborn, A. M., & Clore, G. M. (1995) *Cell 81*, 705−714.

BI951132L